Robust Network Hardening Strategy for Enhancing Resilience of Integrated Electricity and Natural Gas Distribution Systems Against Natural Disasters

Chuan He, *Student Member*, *IEEE*, Chenxi Dai, *Student Member*, *IEEE*, Lei Wu, *Senior Member*, *IEEE*, Tianqi Liu, *Senior Member*, *IEEE*

Abstract—**Recent revolution of the electricity distribution sector, especially a deeper penetration of gas-fired distributed generations (DG), intensifies the interdependence of electricity on natural gas distribution systems. Such integrated electricity and natural gas distribution systems (IENDS) are facing with significant threats from frequent natural disasters that cause enormous economic losses. Network hardening is regarded as an effective technique for enhancing resilience of IENDSs against natural disasters. This paper presents a tri-level robust optimization-based network hardening model for minimizing worst-case total weighted electricity and gas load shedding of IENDSs with respect to hardening budget limits and random damages caused by disasters of different severity levels. Specifically, distinct failure probabilities of overhead power lines and underground gas pipelines are considered, while DGs and gas storages are modeled as effective emergency response resources for supplying high-priority electricity/gas loads during disasters. The proposed model is solved by a column-and-constraint generation (CCG) approach, in which nonlinear gas network constraints are linearized via Taylor series expansion. Numerical case studies evaluate the proposed robust hardening strategy against natural disasters.**

Index Terms— Integrated electricity and natural gas distribution systems, natural disaster, resilience, robust optimization.

NOMENCLATURE

Major symbols and notations used throughout the paper are defined below, while others are defined following their first appearances as needed.

Indices:

b	Index of breakpoints used in the Taylor series expansion.
i, j, k	Indices of power nodes.
(i,j), (m,n)	Indices of power lines and gas pipelines.
l	Index of disaster severity levels.
m, n, o	Indices of natural gas nodes.
t, g	Indices of time periods and DGs.

Sets:

$\boldsymbol{GU}$	Set of gas-fired DGs.
$s(j)$	Set of child nodes of node j.
Ω_j, Ω_n	Set of assets connected to power/gas node j/n.
Ω_B,Ω_D,Ω_L	Sets of power nodes, DGs, and power lines.
Ω_N,Ω_C,Ω_P	Sets of gas nodes, compressors, and pipelines.
Ω_S, Ω_R	Sets of gas storages and gas retailers.

Variables:

$a_{ij,t}$, $a_{mn,t}$	Binary variable which is 1 if power line (i,j)/ gas pipeline (m,n) is available at time t, being 0 otherwise.
$E_{n,t}^{\mathrm{GS}}$	Gas volume of a gas storage at gas node n at time t.
$G_{mn,t}$	Gas flow of pipeline (m,n) at time t.
$G_{n,t}^{\mathrm{GS}}$, $G_{n,t}^{\mathrm{RE}}$	Gas flow injection of gas storage/retailer at gas node n at time t.
$G_{n,t}^{\mathrm{dis}}$, $G_{n,t}^{\mathrm{cha}}$	Gas discharge/charge of a gas storage at gas node n at time t.
h_{ij}, h_{mn}	Binary variable which is 1 if power line (i,j)/ gas pipeline (m,n) is hardened, being 0 otherwise.
NB	Total number of breakpoints used in the Taylor series expansion.
$P_{ij,t}$, $Q_{ij,t}$	Active/reactive power flow of line (i,j) at time t.
$P_{g,t}^{\mathrm{DG}}$, $Q_{g,t}^{\mathrm{DG}}$	Active/reactive power dispatch of DG g at time t.
u_{ij}, u_{mn}	Binary variable which is 1 if power line (i,j)/ gas pipeline (m,n) is damaged by natural disasters, being 0 otherwise.
$V_{j,t}$	Nodal voltage magnitude of bus j at time t.
$\delta_{j,t}$, $\delta_{n,t}$	Load shedding of power/gas node j/n at time t.
$\pi_{n,t}$	Pressure of gas node n at time t.

Constants:

$G_{n,t}^{\mathrm{LD}}$	Gas demand of gas node n at time t.
κ_{ij}, κ_{mn}	Coefficient of hardening effort of power line (i,j)/ gas pipeline (m,n).
K_{mn}	Gas flow constant of gas pipeline (m,n).
M	A large enough positive number.
$p_{ij,l}$, $p_{mn,l}$	Failure probability of power line (i,j)/ gas pipeline (m,n) under disaster severity level l.
$P_{j,t}^{\mathrm{LD}}$, $Q_{j,t}^{\mathrm{LD}}$	Active/reactive power demand of node j at time t.
r_{ij}, x_{ij}	Resistance/reactance of power line (i,j).
T^{enter}	Time point when natural disaster attacks the system.
V_0	Reference voltage magnitude at the substation.
θ_j, θ_n	Priority weight of power load j/gas load n.
Δ_h	Hardening budget.
Δ_l	System parameter corresponding to disaster severity level l.
η_g	Gas fuel consumption factor of gas-fired DG g.
η_{mn}	Fuel consumption factor of a gas compressor at pipeline (m,n).
Γ_{mn}	Compressor factor at pipeline (m,n).
$(\cdot)^{\mathrm{min/max}}$	Min/max value of a quantity.

This work was supported in part by the U.S. National Science Foundation grants ECCS-1254310 and CMMI-1635339. C. He and T. Liu are with the College of Electrical Engineering and Information Technology, Sichuan University, Chengdu, 610065, China (e-mail: jokerscu@stu.scu.edu.cn, tqliu@scu.edu.cn). C. Dai and L. Wu are with the ECE Department, Clarkson University, Potsdam, NY, 13699, USA (e-mail: daic@clarkson.edu, lwu@clarkson.edu).

I. INTRODUCTION

An increasing frequency of catastrophic natural disasters, such as hurricanes and windstorms, has inflicted major social and financial impacts at national, regional, and local levels. Such catastrophic events could result in loss of life and residences, long-term health consequences, and significant impacts on businesses. For instance, in October 2012, the Hurricane Sandy swept the Northeast U.S., causing 147 direct deaths and at least $50 billion worth of damage in the area [1].

One critical issue associated with such disaster events is the availability of electricity for recovery and reconstruction efforts. Reference [2] reviewed impacts of various types of natural disasters that have caused widespread blackouts and affected resilience of power systems. According to a report by the National Oceanic and Atmospheric Administration, the U.S. has sustained 188 weather and climate disasters since 1980, more than 80% of which have brought damages to the nation's electricity infrastructure [3]. The most notable example is the Hurricane Sandy in 2012, which damaged electricity transmission/distribution infrastructures by devastating wind/flood and caused over 8 million customer outages [4]. As a result, reference [5] proposed a probabilistic model to assess resilience of power systems against hurricanes and ensure rapid recovery of power systems from cascading failures.

Electricity grid hardening is regarded as one of the most effective ways for enhancing system resilience against natural disasters [6]-[8]. These hardening techniques, including upgrading poles with guy wires, burying power lines underground, managing vegetation, and elevating substations/ control rooms, can be implemented to protect the power grid against strong wind and flood [8]. However, existing researches [9]-[11] focus on hardening transmission networks against natural disasters, while actually about 90% of weather related outages occur at the distribution level, as indicated in a report by the Executive Office of the President [6]. Thus, enhancing resilience of distribution systems against natural events is becoming a primary task of utilities. A few studies discussed enhancing resilience of distribution systems [12]-[15]. A vegetation maintenance scheduling for overhead power distribution systems was proposed in [12]. Reference [13] studied targeted hardening strategies to protect distribution systems against hurricanes, while considering failure probabilities of power poles. A resilient distribution network planning model was proposed in [14] to coordinate network hardening and distributed generation (DG) allocation. Reference [15] focused on different hardening techniques to protect distribution networks against extreme weather events.

Furthermore, an increasing penetration of gas-fired DGs has significantly intensified the dependency of electricity distribution system on natural gas distribution network [16]. Consequently, extreme weather events, by triggering damages of gas distribution pipelines, could cause further catastrophic outages on power distribution systems. In fact, the Hurricane Sandy caused severe damages to gas distribution pipelines, affecting approximately 32,000 customers of New Jersey Natural Gas [4]. In turn, reference [17] proposed a performance index to measure functionality of the natural gas network against natural disasters. Gas pipelines could be hardened by securing cooling towers, improving tank integrity against wind, and building/strengthening berms/levees/floodwalls against flood.

Impacts of hurricanes on electricity and natural gas systems were thoroughly studied in [18] where a network flow model was adopted to simulate large-scale disruptions. Furthermore, a resilience assessment framework for interdependent electricity and natural gas system was studied in [19] to analyze the joint restoration processes. Indeed, during a natural disaster, resilience of power system and natural gas system is highly interdependent. That is, loss of a power line or shutdown of a pipeline could easily spread to the other system and further lead to cascading failures [18]-[19]. However, researches that explore resilience enhancement of the integrated energy systems are rather limited. Reference [20] proposed to enhance resilience of the power grid via an expansion planning of integrated electricity and natural gas system. A defense strategy to identify and protect vulnerable components was proposed in [21] for increasing resilience of integrated gas-electric system against malicious attacks. However, these works [20]-[21] mainly focus on resilience enhancement of integrated systems at the transmission level, while such a resilience issue for integrated electricity and natural gas distribution systems (IENDS) has not been studied. To fill the gap, this paper proposes a tri-level robust optimization-based network hardening strategy for IENDSs, which identifies the most effective hardening strategy of electric distribution lines and gas distribution pipelines for minimizing electricity and natural gas load shedding (LS) against natural disasters. Compared to [20], the proposed model focuses on hardening strategies of the integrated electricity and natural gas system to protect important components against natural disasters. Compared to [21] which focuses on malicious attacks, this paper concentrates on the modeling of natural disasters and the corresponding optimal hardening strategies. Specifically, in the proposed hardening model, DGs and gas storages are considered as emergency response resources for supporting high-priority loads after system components are damaged by natural disasters. This practical consideration is driven by the facts that: (i) DGs are commonly used as backup generators for providing continued power supply when the main grid is interrupted [22]-[23], while gas-fired DGs further couple electricity and gas distribution systems; and (ii) Gas storage assets can be used as an insurance for maintaining adequate gas network pressure against unforeseen accidents [24].

Furthermore, in reality, as underground pipelines are much more reliable than overhead power lines [25], Claude Shannon's concept of information [15] is adopted in this paper to address distinct failure probabilities of power lines and pipelines. Moreover, the proposed tri-level robust model is solved by a column-and-constraint generation (CCG) algorithm [26], while the lower-level nonlinear dispatch problem is converted into a linear programming (LP) problem by linearizing Weymouth gas flow equations via Taylor series expansion [27].

Major contributions of the paper are twofold.

1) *Integrated Robust Network Hardening Strategy*: The proposed tri-level robust optimization model explores network hardening strategies of IENDS, while considering DGs and gas storage assets as emergency response resources to support

high-priority electricity/gas loads and reduce system LS against natural disasters. In addition, distinct failure probabilities of underground gas pipelines and overhead power lines are considered by recognizing the fact that underground gas pipelines are more reliable.

2) *Solution Algorithm*: Taylor series expansion is applied to linearize nonlinear gas flow equations, which enables dualizing lower-level subproblem of the proposed robust model and facilitates its calculation via CCG algorithm. Two metrics are introduced to examine approximation accuracy of Taylor series expansion. Moreover, a dynamic procedure is proposed to successively add new breakpoints as needed, for deriving high-quality solutions or even global optimal solutions to the original problem with nonlinear gas flow equations.

The rest of the paper is organized as follows. Sections II-III discuss the proposed robust optimization-based network hardening model and solution approach for IENDSs. Numerical case studies are presented in Section IV, and Section V concludes the paper.

II. Model Description

As we do not exactly know how the IENDS will be affected by natural disasters, such uncertainties should be properly simulated in the hardening framework. Stochastic programming and robust optimization are two widely used optimization approaches for handling uncertainties. As power line and pipeline failures against a natural disaster could be completely random, stochastic optimization can be adopted to model natural disasters and their random impacts on system components [10]. In these stochastic models, damage scenarios of natural disasters are modeled as a set of stochastic events with a subset of predefined components that may fail. However, stochastic optimization usually considers high-probability scenarios as a tradeoff between computational time and solution quality. Consequently, neglecting low-probability/ high-damage scenarios in stochastic optimization approaches could bring significant damages to the IENDS. In comparison, robust optimization has become a popular tool to optimize against the worst-case scenarios and control the worst-case damages. In turn, this paper adopts a robust optimization model to anticipate and prepare for the worst-case outcomes of natural disasters.

In the proposed robust network hardening model for enhancing resilience of IENDS against natural disasters, the following assumptions are made.

1) Hardened power distribution lines and gas distribution pipelines will survive natural disasters [9]-[12], [14]. Whereas, once a power line or a gas pipeline is damaged by natural disasters, it will remain unavailable throughout catastrophic events. As this paper mainly focuses on network hardening while DGs, compressors, and gas storages could be more resilient than power lines and gas pipelines [14], [24], [28], they are assumed to survive natural disasters and can be readily used as emergency response resources during catastrophic events.

2) Both electricity and gas distribution networks are radial [14], [29]-[31]. That is, directions of power and gas flows are pre-specified. Consequently, emergency response resources will only be able to supply electricity/gas loads that are connected to the same or their child nodes.

3) Gas fuel consumption of a gas-fired DG only depends on its active power output [32], [33]. Gas fuel consumption of a gas compressor is linearly dependent on gas flow through it [34].

The proposed network hardening model for IENDSs is formulated as a tri-level robust optimization problem (1), which seeks for optimal network hardening plans to minimize the worst-case total weighted electricity and gas LS. Specifically, the upper level determines proactive optimal network hardening strategy in response to upcoming natural disasters, the middle level identifies maximum damages of IENDS caused by natural disasters, and the lower level explores reactions of distribution system operators for minimizing the total weighted LS (TWLS) in response to natural disasters. Weights of individual electricity and gas loads are set based on their priorities. In addition, power LS quantities are multiplied by β/HHV to convert to the same unit of kcf as gas LS, where energy conversion factor β=3.4MBtu/MWh and HHV=1.026 MBtu/kcf [35]-[36].

$$\min_{\boldsymbol{h}\in\boldsymbol{H}}\max_{\boldsymbol{u}\in\boldsymbol{U}}\min_{\boldsymbol{z}\in\boldsymbol{F}(\boldsymbol{h},\boldsymbol{u})}\sum_t\left[\sum_j(\beta/\mathrm{HHV})\cdot\theta_j\cdot\delta_{j,t}+\sum_n\theta_n\cdot\delta_{n,t}\right] \tag{1}$$

where $\boldsymbol{H}$ represents the feasibility set of hardening decisions; $\boldsymbol{U}$ is uncertainty set of network damages caused by natural disasters; $\boldsymbol{F}$ represents feasible IENDS operation conditions; $\boldsymbol{h}$, $\boldsymbol{u}$, and $\boldsymbol{z}$ are vectors of hardening strategies, uncertain network damage statuses with respect to natural disasters, and IENDS operation decision variables.

A. Upper-Level Constraints

Feasibility set of hardening decisions in the upper level is described as in (2), which restricts total hardening efforts within the hardening budget Δ_h. Coefficients κ_{ij} and κ_{mn} indicate distinct levels of efforts/costs required to harden different types of network assets (i.e., overhead power lines and underground pipelines) with different lengths. These values could be determined via the following two ways: (i) coefficients are associated with real-world hardening costs, i.e., similar to reference [15], utilities determine how much money is needed to harden a certain power line or pipeline, while Δ_h represents the total monetary hardening budget; and (ii) coefficients are associated with manpower, i.e., based on historical data utilities can estimate how much manpower is needed to harden a certain power line or pipeline, while Δ_h represents the total manpower hardening budget. In case studies of this paper, hardening coefficients of power lines and gas pipelines are set as 1 and 3 to replicate practical situations, indicating that hardening an underground pipeline needs two times more money/manpower than an overhead power line.

$$\boldsymbol{H}=\left\{\boldsymbol{h}:\sum_{(i,j)\in\Omega_L}\kappa_{ij}\cdot h_{ij}+\sum_{(m,n)\in\Omega_P}\kappa_{mn}\cdot h_{mn}\le\Delta_h, h_{ij},h_{mn}\in\{0,1\}\right\} \tag{2}$$

B. Middle-Level Constraints

Middle-level constraints describe uncertainty sets of random damages caused by natural disasters. Indeed, various natural disasters present unique characteristics and could affect power grid and natural gas network to varying degrees. As pointed in

[2], predictability, impacted region, and affecting time of individual natural disasters are different. In literature [2], [10], [14]-[15], researchers typically model impact of different types of natural disasters via the number of system components that are damaged. Follow the tradition, this paper also uses number of system component outages to model the impact of different types of natural disasters. Consequently, by considering different numbers of system components at fault, the model presented in this paper can apply to different types of natural disasters, including weather related natural disasters and other non-weather related natural disasters such as earthquake that could impact power grid and natural gas network.

Indeed, considering that natural gas is an important primary energy resource, outage of a gas pipeline by natural disasters could lead to cascading outages of multiple gas-fired DGs, and result in extensive power LS of an electricity distribution network. On the other hand, because underground pipelines are much more reliable than overhead power lines, conventional uncertainty set modeling of power lines such as N-K contingency may not be applicable [9]-[11], [14]-[15]. In this paper, according to Claude Shannon's concept of information [15], coefficients $-\log_2 p_{ij,l}$ and $-\log_2 p_{mn,l}$ are used to represent distinct resilience characteristics of individual power lines and gas pipelines under disaster severity level l. For instance, taking an overhead power line with a failure probability of 0.3 and an underground gas pipeline with a failure probability of 0.1 as an example, coefficients of the power line and gas pipeline are respectively 1.737 and 3.32, i.e., it takes much more efforts to damage a more resilient pipeline. It is noted that failure probability considered in the model refers to probability that a component will fail during natural disasters in a short term, which is different from failure rate or forced outage rate (FOR) used in the long-term reliability assessment [37]. For different types of natural disasters, utilities can calculate failure probabilities of overhead power lines $\bar{p}_{ij,l}$ and underground pipelines $\bar{p}_{mn,l}$ at severity level l. Failure probabilities of overhead systems can be calculated using equations in reference [5], [38]. Similarly, for underground systems, their failure probabilities can be calculated via approach in [15], [39] Given failure probabilities of different components with respect to a certain natural disaster, the proposed model can identify effective hardening strategies against this type of natural disasters.

Middle-level constraints are presented as in (3)-(7). Constraint (3) describes extend of random damages caused by natural disasters, where $\left(-\log_2 \Delta_l\right)$ represents budget of system component failures corresponding to disaster severity level l. One possible way to determine this parameter Δ_l is through expected maximum numbers of power line and pipeline outages and their corresponding average failure probabilities. That is, (i) From historical data or by expectation, determine numbers of power lines K_p and pipelines K-K_p that could fail in a natural disaster of severity level l; (ii) Calculate average failure probabilities of individual power lines $\bar{p}_{ij,l}$ and pipelines $\bar{p}_{mn,l}$ in a natural disaster of severity level l using their individual failure probabilities; and (iii) Calculate system parameter Δ_l via $\Delta_l=\bar{p}_{ij,l}^{K_p}\cdot\bar{p}_{mn,l}^{(K\text{-}K_p)}$. It is also noteworthy that K_p and K-K_p are pre-specified for calculating Δ_l only, while worst-case power line and pipeline failures will be determined by the proposed model according to Δ_l and their importance to the IENDS. The proposed method is an extension of the traditional N-K criterion. That is, if failure probabilities of power lines and pipelines are the same, equation (3) will degrade to the traditional N-K criterion which defines that at most K power lines and pipelines will fail. Constraint (4)-(5) describes that power lines and pipelines are available before catastrophic events. Equations (6)-(7) represent logic relationships among availability a, hardening h, and damages by natural disasters u for individual power lines and pipelines after catastrophic events. (8) imposes binary restrictions on a and u variables. The component failure model (3)-(8) could be extended to consider different numbers of failure components in different time slots during the disaster, if information on dynamics of disasters sweeping the area can be reasonably obtained and the distribution system spans a larger area that will not be influenced by the disaster at the same time.

$$\boldsymbol{U}=\Big\{\boldsymbol{u}: \textstyle\sum_{(i,j)\in\Omega_L}\left(-\log_2 p_{ij,l}\right)\cdot u_{ij}+\sum_{(m,n)\in\Omega_P}\left(-\log_2 p_{mn,l}\right)\cdot u_{mn} \leq -\log_2 \Delta_l \quad (3)$$

$$a_{ij,t}=1, \qquad t<T^{\text{enter}},(i,j)\in\Omega_L \quad (4)$$

$$a_{mn,t}=1, \qquad t<T^{\text{enter}},(m,n)\in\Omega_P \quad (5)$$

$$a_{ij,t}=1-u_{ij}+u_{ij}\cdot h_{ij}, \qquad t\geq T^{\text{enter}},(i,j)\in\Omega_L \quad (6)$$

$$a_{mn,t}=1-u_{mn}+u_{mn}\cdot h_{mn}, \qquad t\geq T^{\text{enter}},(m,n)\in\Omega_P \quad (7)$$

$$u_{ij},u_{mn},a_{ij,t},a_{mn,t}\in\{0,1\}, \qquad (i,j)\in\Omega_L,(m,n)\in\Omega_P\Big\} \quad (8)$$

C. Lower-Level Constraints

Lower-level constraints (9)-(29) describe physical operation conditions of IENDSs. For an electricity distribution network, the linearized DistFlow model is adopted to calculate complex power flows [14]-[15], [40]. Specifically, active and reactive power flow balances are enforced via (9)-(10). Branch voltage differences and branch power flows are limited as in (11)-(13) with respect to network connectivity indicator $a_{ij,t}$. Limits on DG outputs as well as voltage levels and electrical LS of individual nodes are enforced in (14)-(17). Although convex relaxations, such as second-order cone programing (SOCP), of nonlinear Distflow model have been recently explored in literature, they may not be applicable in the proposed model. The reason is that in order to ensure solution exactness of convex relaxation, the objective function needs to be formulated as minimizing total costs or losses [41]-[42], while the objective of this paper is to minimize TWLS of the IENDS. In addition, the linearized DistFlow model has been widely used in various distribution system applications including optimal DG placement [30], service restoration [28], and optimal operation [43], while its solution quality has also been extensively studied in literature.

Constraints (18)-(29) describe Weymouth gas flow equations and operation characteristics of a natural gas distribution network. As demonstrated in Fig. 1, gas network nodal balance equation (18) represents that the total gas flow injection from $G_{mn,t}$, $G_{n,t}^{\mathrm{GS}}$, and $G_{n,t}^{\mathrm{RE}}$ is equal to the total gas withdrawn by $G_{no,t}$, $G_{n,t}^{\mathrm{LD}}$, $\left(\eta_g \cdot P_{g,t}^{\mathrm{DG}}\right)$, and $\left(\eta_{mn} \cdot G_{mn,t}\right)$ at each gas node. Fuel consumption factor of gas compressor η_{mn} is set as 0.03-0.05 based on the fact that a gas compressor usually consumes about 3-5% of the total transported gas [34]. Coefficient η_g is calculated as $\beta/\left(\mathrm{HHV} \cdot e_g^{\mathrm{DG}}\right)$, where e_g^{DG} is efficiency of DG g. As gas flow directions in the natural gas distribution network are pre-specified, Weymouth gas flow equation of a gas pipeline is described as in (19) [44]. Analogous to power flows of power lines, gas flows of pipelines are also constrained by their capacity limits (20). In addition, (21) describes that two terminal pressures of a gas compressor are limited by compressor factor Γ_{mn} [27]. Constraint (22) describes pressure limits of individual gas nodes. Operation limits of gas storage facilities are presented as in (23)-(26), including net gas output, capacity balance, as well as lower/upper limits of discharge/charge rate and storage capacity. Finally, constraints (28)-(29) impose limits on supply capabilities of gas retailers and gas LS.

$$\boldsymbol{F}=\Big\{\boldsymbol{z}\colon \textstyle\sum_{k\in s(j)} P_{jk,t}=P_{ij,t}-P_{j,t}^{\mathrm{LD}}+\sum_{g\in\Omega_j} P_{g,t}^{\mathrm{DG}}+\delta_{j,t}, \qquad j\in\Omega_B \quad (9)$$

$$\textstyle\sum_{k\in s(j)} Q_{jk,t}=Q_{ij,t}-Q_{j,t}^{\mathrm{LD}}+\sum_{g\in\Omega_j} Q_{g,t}^{\mathrm{DG}}+\left(\delta_{j,t}/P_{j,t}^{\mathrm{LD}}\right)\cdot Q_{j,t}^{\mathrm{LD}}, j\in\Omega_B \quad (10)$$

$$-\left(1-a_{ij,t}\right)\cdot M\le V_{i,t}-V_{j,t}-\left(r_{ij}\cdot P_{ij,t}+x_{ij}\cdot Q_{ij,t}\right)/V_0\le\left(1-a_{ij,t}\right)\cdot M, \qquad (i,j)\in\Omega_L \quad (11)$$

$$0\le P_{ij,t}\le a_{ij,t}\cdot P_{ij}^{\max}, \qquad (i,j)\in\Omega_L \quad (12)$$

$$0\le Q_{ij,t}\le a_{ij,t}\cdot Q_{ij}^{\max}, \qquad (i,j)\in\Omega_L \quad (13)$$

$$0\le P_{g,t}^{\mathrm{DG}}\le P_g^{\mathrm{DG,max}}, \qquad g\in\Omega_D \quad (14)$$

$$0\le Q_{g,t}^{\mathrm{DG}}\le Q_g^{\mathrm{DG,max}}, \qquad g\in\Omega_D \quad (15)$$

$$V_j^{\min}\le V_{j,t}\le V_j^{\max}, \qquad j\in\Omega_B \quad (16)$$

$$0\le \delta_{j,t}\le P_{j,t}^{\mathrm{LD}}, \qquad j\in\Omega_B \quad (17)$$

$$\textstyle\sum_{o\in s(n)} G_{no,t}=G_{mn,t}-G_{n,t}^{\mathrm{LD}}-\sum_{g\in\Omega_n}\eta_g\cdot P_{g,t}^{\mathrm{DG}}-\sum_{(m,n)\in\Omega_C}\eta_{mn}\cdot G_{mn,t}+G_{n,t}^{\mathrm{GS}}+G_{n,t}^{\mathrm{RE}}+\delta_{n,t}, n\in\Omega_N \quad (18)$$

$$-\left(1-a_{mn,t}\right)\cdot M\le G_{mn,t}-K_{mn}\cdot\sqrt{\pi_{m,t}^2-\pi_{n,t}^2}\le\left(1-a_{mn,t}\right)\cdot M, \qquad (m,n)\in\Omega_P \quad (19)$$

$$0\le G_{mn,t}\le a_{mn,t}\cdot G_{mn}^{\max}, \qquad (m,n)\in\Omega_P \quad (20)$$

$$\pi_{n,t}\le\Gamma_{mn}\cdot\pi_{m,t}, \qquad (m,n)\in\Omega_C \quad (21)$$

$$\pi_n^{\min}\le\pi_{n,t}\le\pi_n^{\max}, \qquad n\in\Omega_N \quad (22)$$

$$G_{n,t}^{\mathrm{GS}}=G_{n,t}^{\mathrm{dis}}-G_{n,t}^{\mathrm{cha}}, \qquad n\in\Omega_S \quad (23)$$

$$E_{n,t}^{\mathrm{GS}}=E_{n,t\text{-}1}^{\mathrm{GS}}-G_{n,t}^{\mathrm{GS}}, \qquad n\in\Omega_S \quad (24)$$

$$G_n^{\mathrm{GS,min}}\le G_{n,t}^{\mathrm{dis}}\le G_n^{\mathrm{GS,max}}, \qquad n\in\Omega_S \quad (25)$$

$$G_n^{\mathrm{GS,min}}\le G_{n,t}^{\mathrm{cha}}\le G_n^{\mathrm{GS,max}}, \qquad n\in\Omega_S \quad (26)$$

$$E_n^{\min}\le E_{n,t}^{\mathrm{GS}}\le E_n^{\max}, \qquad n\in\Omega_S \quad (27)$$

$$0\le G_{n,t}^{\mathrm{RE}}\le G_n^{\mathrm{RE,max}}, \qquad n\in\Omega_R \quad (28)$$

$$0\le \delta_{n,t}\le G_{n,t}^{\mathrm{LD}}, \qquad n\in\Omega_N\Big\} \quad (29)$$

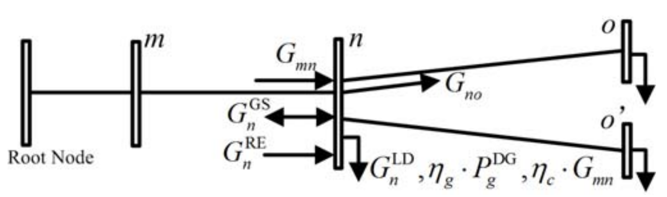

Fig. 1 An illustrative radial natural gas distribution network

III. Solution Methodology

In this paper, we use CCG to solve the proposed tri-level min-max-min robust hardening problem (1)-(29), which has been widely used for solving robust optimization instances [26], [32]. Moreover, this paper adopts Taylor series expansion to linearize Weymouth gas flow equation (19) [27], [45], which converts the lower-level minimization problem to an LP to facilitate the implementation of CCG.

A. Linearize Weymouth Gas Flow Equations

In this subsection, the original Weymouth equation while considering outages of pipelines (19) is discussed via two situations, i.e., a pipeline is available $a_{mn,t}$=1 and is on outage $a_{mn,t}$=0.

(i) When $a_{mn,t}$=1, equation (19) reduces to the standard Weymouth equation as described in (30). Applying Taylor series expansion, linear outer approximation of (30) around certain given terminal pressures $\left(\hat{\pi}_{m,t},\hat{\pi}_{n,t}\right)$ is given as in (31) [27], [45].

$$G_{mn,t}=K_{mn}\cdot\sqrt{\pi_{m,t}^2-\pi_{n,t}^2}, \qquad (m,n)\in\Omega_P \quad (30)$$

$$G_{mn,t}\le K_{mn}\cdot\sqrt{\hat{\pi}_{m,t}^2-\hat{\pi}_{n,t}^2}+\frac{\partial G_{mn,t}}{\partial\pi_{m,t}}\cdot\left(\pi_{m,t}-\hat{\pi}_{m,t}\right)+\frac{\partial G_{mn,t}}{\partial\pi_{n,t}}\cdot\left(\pi_{n,t}-\hat{\pi}_{n,t}\right) \qquad (m,n)\in\Omega_P \quad (31)$$

Let us define NB pairs of breakpoints $\left(\hat{\pi}_{m,t}^b,\hat{\pi}_{n,t}^b\right)$ with $\hat{\pi}_{m,t}^b>\hat{\pi}_{n,t}^b$ for b=1,2,…, NB, $\pi_m^{\min}\le\hat{\pi}_{m,t}^1\le\ldots\le\hat{\pi}_{m,t}^{NB}\le\pi_m^{\max}$, and $\pi_n^{\min}\le\hat{\pi}_{n,t}^1\le\ldots\le\hat{\pi}_{n,t}^{NB}\le\pi_n^{\max}$. It is pointed out in [27] that each plane, given by (32)-(34) corresponding to a pair of breakpoints, is tangent to the cone described by (30) at a line where the ratio between intake pressure $\pi_{m,t}$ and outtake pressure $\pi_{n,t}$ is equal to the ratio between $\hat{\pi}_{m,t}^b$ and $\hat{\pi}_{n,t}^b$. In turn, all planes in the form of (32)-(34) corresponding to all NB pairs of breakpoints represent an outer approximation of cone described by the original Weymouth equation (30) in the entire region of $\pi_n^{\min}\le\pi_{n,t}\le\pi_n^{\max}$ and $\pi_m^{\min}\le\pi_{m,t}\le\pi_m^{\max}$ [27], [45].

$$G_{mn,t}\le K_{mn}\cdot\hat{\varphi}_{mn,t}^b\cdot\pi_{m,t}-K_{mn}\cdot\hat{\phi}_{mn,t}^b\cdot\pi_{n,t}, \qquad (m,n)\in\Omega_P \quad (32)$$

$$\pi_{m,t}\ge\pi_{n,t}, \qquad (m,n)\in\Omega_P \quad (33)$$

$$\hat{\varphi}_{mn,t}^b=\hat{\pi}_{m,t}^b/\sqrt{\left(\hat{\pi}_{m,t}^b\right)^2-\left(\hat{\pi}_{n,t}^b\right)^2}\ ;\ \hat{\phi}_{mn,t}^b=\hat{\pi}_{n,t}^b/\sqrt{\left(\hat{\pi}_{m,t}^b\right)^2-\left(\hat{\pi}_{n,t}^b\right)^2} \quad (34)$$

(ii) When $a_{mn,t}$=0, the original Weymouth equation considering random outages (19) is not binding and always satisfied. That is, under this situation, equation (20) restricts gas flow of this pipeline to zero, and (32)-(34) are always satisfied.

In summary, constraints (32)-(34) can be used to equivalently replace equation (19), and constraints (20) and (32)-(34) all together represent a valid linear approximation of the original Weymouth equation while considering outages of pipelines.

B. CCG Solution Algorithm

For the sake of discussion, the proposed tri-level robust optimization problem with linearized Weymouth gas flow equations is rewritten in a compact form as in (35).

$$\min_{\boldsymbol{h}\in\boldsymbol{H}}\max_{\boldsymbol{u}\in\boldsymbol{U}}\min_{\boldsymbol{z}\in\boldsymbol{F}(\boldsymbol{h},\boldsymbol{u})} \boldsymbol{c}^{\mathrm{T}}\boldsymbol{z} \quad (35)$$

where $\boldsymbol{F}(\boldsymbol{h},\boldsymbol{u})=\{z{:}\boldsymbol{C}z+\boldsymbol{D}\boldsymbol{h}+\boldsymbol{E}\boldsymbol{u}\leq\boldsymbol{g}\}$ corresponds to (9)-(18), (20)-(29), and (32)-(34), in which $\boldsymbol{C}$, $\boldsymbol{D}$, and $\boldsymbol{E}$ are constant coefficient matrixes while $\boldsymbol{c}$ and $\boldsymbol{g}$ are constant coefficient vectors.

CCG is employed to solve (35) in a master-subproblem framework [26], [32]. Specifically, by iteratively adding worst-case network damage scenarios $\hat{\boldsymbol{u}}$ identified in the subproblem, master problem (36) yields a network hardening strategy $\hat{\boldsymbol{h}}$ and a lower bound of (35). $\mathbf{W}$ represents the set of worst-case indices iteratively identified in the subproblem.

$$\min_{\boldsymbol{h}\in\boldsymbol{H},\boldsymbol{z}} \sigma$$
$$\text{s.t. } \sigma\geq\boldsymbol{c}^{\mathrm{T}}\boldsymbol{z}_w;\ \ \boldsymbol{C}\boldsymbol{z}_w+\boldsymbol{D}\boldsymbol{h}+\boldsymbol{E}\hat{\boldsymbol{u}}_w\leq\boldsymbol{g}, \qquad \forall w\in\mathbf{W} \tag{36}$$

With a given network hardening strategy $\hat{\boldsymbol{h}}$ from the master problem, the bi-level max-min subproblem (37) identifies the worst-case network damage scenario caused by natural disasters that would lead to the largest TWLS. (37) can be recasted into an equivalent single-level bilinear maximization problem (38) by applying duality theory on the inner LP problem, where $\boldsymbol{\lambda}$ are dual variables of the inner-level LP.

$$\gamma(\hat{\boldsymbol{h}})=\max_{\boldsymbol{u}\in\boldsymbol{U}}\ \min_{\boldsymbol{z}\in\boldsymbol{F}(\boldsymbol{h},\boldsymbol{u})} \boldsymbol{c}^{\mathrm{T}}\boldsymbol{z}$$
$$\text{s.t. } \boldsymbol{C}\boldsymbol{z}+\boldsymbol{D}\hat{\boldsymbol{h}}+\boldsymbol{E}\boldsymbol{u}\leq\boldsymbol{g} : (\boldsymbol{\lambda}) \tag{37}$$
$$\gamma(\hat{\boldsymbol{h}})=\max_{\boldsymbol{u}\in\boldsymbol{U},\boldsymbol{\lambda}}\left(\boldsymbol{g}\text{-}\boldsymbol{D}\hat{\boldsymbol{h}}\text{-}\boldsymbol{E}\boldsymbol{u}\right)^{\mathrm{T}}\boldsymbol{\lambda}$$
$$\text{s.t. } \boldsymbol{C}^{\mathrm{T}}\boldsymbol{\lambda}\leq\boldsymbol{c},\ \boldsymbol{\lambda}\leq 0 \tag{38}$$

Furthermore, bilinear terms in the objective function of (38), e.g. products of binary variables and dual variables $\boldsymbol{u}^{\mathrm{T}}\boldsymbol{\lambda}$, can be equivalently linearized via well-known algebra results [46]. For instance, a bilinear term $u\cdot\lambda$ can be linearized as in (39)-(41) with an ancillary continuous variable r.

$$r=u\cdot\lambda \tag{39}$$
$$-u\cdot M\leq r\leq 0 \tag{40}$$
$$\lambda\text{-}(1\text{-}u)\cdot M\leq r\leq\lambda+(1\text{-}u)\cdot M \tag{41}$$

The detailed solution procedure is summarized as follows.

Step 1) Set lower bound LB=0 and upper bound $UB=\infty$. Initialize convergence tolerance ε, iteration index w=1, and $\mathbf{W}=\emptyset$.

Step 2) Solve master problem (36), derive optimal solution $\hat{\boldsymbol{h}}_w$ and optimal objective value $\hat{\sigma}_w$, and update $LB=\hat{\sigma}_w$.

Step 3) Solve subproblem (38) with respect to $\hat{\boldsymbol{h}}_w$, obtain optimal solution $\hat{\boldsymbol{u}}_w$ and optimal objective value $\gamma(\hat{\boldsymbol{h}}_w)$, and update $UB=\min\{UB,\gamma(\hat{\boldsymbol{h}}_w)\}$.

Step 4) If $UB\text{-}LB\leq\varepsilon$, terminate and return optimal solution $\hat{\boldsymbol{h}}_w$. Otherwise, add new variables $\boldsymbol{z}_w$ as well as new constrains $\sigma\geq\boldsymbol{c}^{\mathrm{T}}\boldsymbol{z}_w$ and $\boldsymbol{C}\boldsymbol{z}_w+\boldsymbol{D}\boldsymbol{h}+\boldsymbol{E}\hat{\boldsymbol{u}}_w\leq\boldsymbol{g}$ into master problem (36), update $\mathbf{W}=\mathbf{W}\cup\{w\}$ and w=w+1, and go back to Step 2.

C. Discussion on Accuracy of Taylor Series Expansion based Outer Approximation

In above Sections III.A-B, Weymouth equation (19) is approximated by a set of linear inequalities via Taylor series expansion, which could potentially introduce calculation error and derive solutions that are infeasible to (19). Specifically, if optimal nodal gas pressures calculated from (36) and (38) are not identical to any breakpoint, the solution may not satisfy (19) and infeasible to the original problem. On the other hand, if optimal nodal gas pressures from (36) and (38) are identical to certain breakpoints, linearization (32)-(34) is exact and the derived solution is optimal [45]. That is, the closer to breakpoints the resulting nodal pressures are, the more exact the linearization is. Consequently, increasing the number of breakpoints could improve accuracy of approximation [47].

In Step 3 of Section III.B, the subproblem is solved in one-shot with a predefined fixed number of breakpoints. Although there is a good chance that the solution is of good quality when the number of breakpoints is sufficiently large, it is still necessary to examine solution quality for ensuring that approximation error is within an acceptable range. Thus, the following iterative procedure is proposed to extend Step 3 of Section III.B, which dynamically adds additional breakpoints for identifying high-quality solutions to the original Weymouth equation (19). In this dynamic procedure, an upper bound and a lower bound are iteratively calculated to examine solution quality of the lower-level dispatch problem through Taylor series expansion. The same procedure is applicable to the master problem (36). Note that the following procedure intends to boost approximation accuracy of Taylor series expansion in the lower-level subproblem. Essentially, gas flows in pipelines are approximated through (32)-(34) and the lower-level dispatch problem tries to maximize gas flows to support gas loads. Thus, if gas flow approximations are of high quality, possibly exact, gas load shedding in (37) corresponding to pipeline outages can be accurately approximated. Furthermore, damaged pipelines instead of total gas load shedding are of concern, which may not be sensitive to approximation errors. In turn, pipeline outage solutions of problem (38) are considered good enough.

Step 3.1) Solve subproblem (38) via Taylor series expansion to obtain availability status of power lines $a^*_{ij,t}$ and pipelines $a^*_{mn,t}$.

Step 3.2) Solve the lower-level dispatch subproblem of (37) with $a^*_{ij,t}$ and $a^*_{mn,t}$ to retrieve gas flow solution $G^*_{mn,t}$. The optimal objective value is denoted as lower bound LB^{gf} of the original nonlinear lower-level dispatch subproblem.

Step 3.3) Solve (42) with $G^*_{mn,t}$, $a^*_{ij,t}$, and $a^*_{mn,t}$, and the optimal objective value is denoted as UB^{gf}.

$$\operatorname{Min}\sum\nolimits_t\begin{pmatrix}\sum_j(\beta/\mathrm{HHV})\cdot\theta_j\cdot\delta_{j,t}+\sum_n\theta_n\cdot\delta_{n,t}\\ +\rho\cdot\sum_{(m,n)\in\Omega_P}\left(\xi^+_{mn,t}+\xi^-_{mn,t}\right)\end{pmatrix}$$
$$\text{s.t. } \text{-}\left(1\text{-}a^*_{mn,t}\right)\cdot M\leq\left(G^*_{mn,t}\right)^2\text{-}K^2_{mn}\cdot\left(\pi^2_{m,t}\text{-}\pi^2_{n,t}\right)+\xi^+_{mn,t}\text{-}\xi^-_{mn,t}$$
$$\leq\left(1\text{-}a^*_{mn,t}\right)\cdot M,\ (m,n)\in\Omega_P$$
$$\text{Constraints (9)-(18) and (20)-(29).} \tag{42}$$

In (42), potential violation of Weymouth equation (19) with respect to given $G^*_{mn,t}$, $a^*_{ij,t}$ and $a^*_{mn,t}$ is penalized in objective function of the lower-level dispatch subproblem with a positive penalty factor ρ. In addition, squared nodal pressure $\pi^2_{n,t}$ is considered as a single variable. In turn, (42) with given gas flow solution $G^*_{mn,t}$ is an LP problem, and provides an upper bound to the original nonlinear lower-level dispatch subproblem with respect to given $a^*_{ij,t}$ and $a^*_{mn,t}$.

Step 3.4) If either gap between upper bound UB^{gf} and lower bound LB^{gf}, i.e. $\left(UB^{\mathrm{gf}}\text{-}LB^{\mathrm{gf}}\right)/LB^{\mathrm{gf}}\leq\varepsilon^{\mathrm{gf}}$, or the maximum error in the Weymouth equation $Error=\min_{(m,n)\in\Omega_P}\left\{\left(\xi^{+}_{mn,t}+\xi^{-}_{mn,t}\right)/\left(G^{*}_{mn,t}\right)^{2}\right\}\leq\varepsilon^{\mathrm{gf}}$ meets certain threshold, the derived result represents a good-enough solution and the process terminates. Specifically, if lower and upper bounds are equal, the derived result is an optimal solution to the original nonlinear lower-level dispatch subproblem; Otherwise, go to Step 3.5.

Step 3.5) Add additional breakpoints for improving accuracy of approximation, and go back to Step 3.1. It is noteworthy that tuning breakpoints around real operating conditions could reduce the number of breakpoints needed for achieving a same accuracy level. For instance, more breakpoints around nodal pressures obtained from Step 3.3, which represents a good intermediate solution, could be generated.

IV. Numerical Results

The proposed robust network hardening approach is demonstrated on an IENDS consisting of a modified IEEE 33-node electricity distribution grid and a modified 20-node Belgian gas network. As shown in Fig. 2, the IENDS includes 2 gas-fired DGs, 1 non-gas DG, 2 gas retailers, 2 gas storages, 32 power distribution lines, 17 pipelines, 2 gas compressors, 32 power loads, and 15 gas loads. DGs at power nodes 6 and 12 are respectively connected to gas nodes 9 and 14 for gas fuel supply. Voltage limits of all power nodes are set as [0.95, 1.05] p.u. Other system configuration data can be found in [48].

System electrical and gas load profiles are shown in Fig. 3. Electrical and gas loads are divided into 5 priority categories with priority weights θ_j/θ_n from 1 to 5. Thresholds ε and $\varepsilon^{\mathrm{gf}}$ are both 1%. All case studies are solved via Gurobi 6.5.

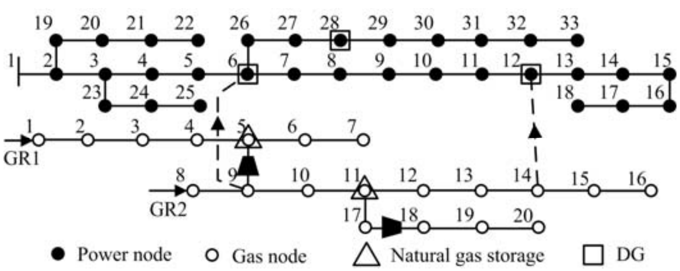

Fig. 2 Power-gas distribution system

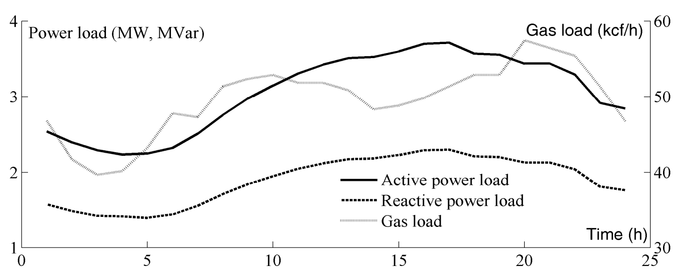

Fig. 3 System electrical and natural gas load profiles

A. Approximation Accuracy of Taylor Series Expansion

The lower-level system dispatch problem is used in this section to investigate approximation accuracy of Taylor series expansion. Penalty factor ρ is set as 1. Two tests are carried out, in which the first test uses original gas flow constants K_{mn} in [48], and the second one reduces K_{mn} to 60% of their original values to trigger gas network congestion. Results against different numbers of breakpoints are reported in Table I.

It is observed that when natural gas network is lightly loaded, i.e., without LS or network congestion, both gap and Weymouth equation error are zeros regardless the number of breakpoints, indicating that obtained solutions are optimal. On the other hand, when gas network with a lower transportation capability is congested, i.e., nodal pressures at certain nodes reach their lower/upper limits, more breakpoints are needed to reasonably approximate optimal gas flows with smaller gaps and errors. Specifically, in this case, 100 breakpoints can reach the predefined error threshold of 1% although gap is still higher than 1%. Moreover, when the number of breakpoints reaches 500, upper bound UB^{gf} is significantly improved, and a higher accurate solution is obtained with gap of 0.71%. It is concluded that a proper number of breakpoints can reasonably enhance approximation accuracy of Taylor series expansion.

TABLE I Approximation Accuracy of Taylor Series Expansion

# of breakpoints	Without congestion				With congestion			
	LB^{gf}	UB^{gf}	Gap(%)	Error(%)	LB^{gf}	UB^{gf}	Gap(%)	Error(%)
50	0	0	0	0	620.83	817.67	31.71	2.32
80	0	0	0	0	627.03	734.50	17.14	1.26
100	0	0	0	0	631.32	676.25	7.12	**0.56**
200	0	0	0	0	633.19	650.24	2.69	0.31
500	0	0	0	0	634.06	638.55	**0.71**	0.14

B. Natural Disasters and Their Worst-case Damages

A 24-hour period is considered to study impacts of a natural disaster hitting the IENDS at hour 8. Parameter settings with respect to disaster severity level l are shown in Table III. Without network hardening, worst-case damages of natural disasters to the original IENDS is obtained by solving max-min subproblem (38). Table III shows worst-case damages by natural disaster with respect to different severity levels while the number of breakpoints is set as 50. Note that as severity level increases, failure probability of each component also increases. Gaps and errors against all severity levels are zeros, indicating that optimal solutions are obtained. Specifically, in this case, since no gas network congestion occurs, a small number of breakpoints is sufficient to guarantee approximation accuracy.

TABLE II Component failure probabilities and System parameter

Severity level	Maximum numbers of expected damages on power lines and gas pipelines	$(p_{ij,l}, p_{mn,l})$	Δ_l
1	(2,0)	(0.2,0.03)	0.04
2	(2,1)	(0.3,0.05)	0.0045
3	(2,2)	(0.4,0.1)	0.0016
4	(3,3)	(0.6,0.13)	0.0004
5	(3,5)	(0.7,0.2)	0.0001

TABLE III Worst-case Damages Against Different Severity Levels

Severity level	Proposed method			N-*K*	
	Damaged components	Damages	TWLS	Damages	TWLS
1	L1-2, L6-7	(2,0)	299.14	(0,2)	2053.45
2	L1-2, L28-29, P8-9	(2,1)	2019.00	(1,2)	2468.31
3	L1-2, L28-29, P1-2, P8-9	(2,2)	2537.94	(1,3)	2718.31
4	L1-2, L6-26, L28-29, P1-2, P5-6, P8-9	(3,3)	2787.94	(1,5)	2967.08
5	L1-2, L6-26, L28-29, P1-2, P5-6, P8-9, P11-12, P11-17	(3,5)	3036.70	(3,5)	3036.70

Table III also shows that a higher severity level induces more component damages with a higher TWLS. As underground pipelines are much more reliable than overhead power lines, they could survive natural disasters of low severity levels. Specifically, a natural disaster with severity level of 1 is not catastrophic enough to damage underground pipelines. When severity level increases to 2, damages on underground pipelines emerge. Moreover, because natural gas is a primary energy resource for both non-generation gas loads and gas-fired DGs, under high-severity natural disasters, damaging the gas distribution network could be more destructive than the electricity distribution grid in terms of a larger TWLS. In fact, in this case, pipeline P8-9 and power line L28-29, instead of power line L6-7 at severity level of 1, are damaged, which significantly increases TWLS by about 575%. Indeed, as the electricity distribution grid depends on the gas distribution network for supplying gas fuel to gas-fired DGs when power supply from the main grid is unavailable, damaging the gas distribution network would potentially restrict power generation of gas-fired DGs and lead to significant electrical LS. Specifically, when pipeline P8-9 is damaged, gas supply to gas-fired DG at power node 6 is cut off, which, together with damage of power line L1-2, leads to a completely outage of power nodes 2-11. As a result, damaging power line L28-29 instead of L6-7 would lead to the worst case with larger TWLS.

The proposed method based on Claude Shannon's concept and the traditional N-*K* criterion are further compared. Results are shown in Table III. At severity level 1 where the natural disaster is not strong enough to damage underground pipelines, results of the proposed method show that two power lines are damaged. In comparison, the N-*K* criterion derives results of two pipeline failures which seem unpractical. Similarly, for severity levels ranging from 2 to 4, the N-K criterion derives a higher total weighted load shedding (TWLS) with more pipelines damaged. Although these N-*K* criterion results correctly indicate the importance of pipelines in the IENDS, they fail to accurately reflect real-world characteristics of overhead power lines and underground pipelines during natural disaster, i.e., underground pipelines are far more resilient than power lines. Finally, results from both methods at severity level 5 are the same, because most of the major components are damaged under this catastrophic disaster level. In summary, the traditional N-*K* criterion is a good way to identify importance of components in the IENDS, but fails to represent practical consequences against actual disaster levels. In comparison, the proposed method based on Claude Shannon's concept, by using different coefficients on overhead power lines and underground pipelines, can accurately simulate real-world situations that underground pipelines are less likely to be damaged than power lines during certain severe levels of natural disasters.

To further investigate potential impacts of different numbers of breakpoints on worst-case damage identification results when gas congestion occurs, gas flow constants K_{mn} of all pipelines are reduced to 60% of their original values. Results against different numbers of breakpoints are shown in Table IV, with disaster severity level of 2. Similar trend as in Table I is observed, i.e., more breakpoints results in a smaller gap/error. That is, more breakpoints will derive a better lower bound of TWLS. On the other hand, it is observed that outages of the same two power lines and one gas pipeline are identified as the worst case with different numbers of breakpoints, while TWLSs obtained from different numbers of breakpoints are also close. In summary, it can be concluded that a reasonably small number of breakpoints could be utilized to enhance computational efficiency while not compromising the proposed approach, since identifying worst-case damaged components is the main concern instead of exact nodal pressure levels.

TABLE IV WORST-CASE DAMAGES WITH DISASTER SEVERITY LEVEL 2

# of breakpoints	Damaged components	TWLS	Gap	Error
30	L1-2, L28-29, P8-9	2107.96	4.95%	31.01%
50	L1-2, L28-29, P8-9	2109.95	2.33%	15.00%
100	L1-2, L28-29, P8-9	2111.57	0.23%	1.61%
200	L1-2, L28-29, P8-9	2111.74	0.01%	0.31%
500	L1-2, L28-29, P8-9	2111.74	0.01%	0.24%

C. Importance of DGs and Natural Gas Storages

It is well recognized that when the main grid power is lost during natural disasters, DGs can serve as emergency response resources in an electricity distribution system for continuously supplying critical electrical loads. Analogously, when main gas supply from gas retailers is down, gas storages in a gas distribution system can be used as emergency resources for supplying high-priority gas loads. The following three cases are studied to investigate importance of DGs and gas storages on resilience of an IENDS, by comparing worst-case TWLSs with respect to different disaster severity levels:

C1: No DGs.
C2: No natural gas storages.
C3: No DGs and natural gas storages.

Results in Table IV show that a higher disaster severity level derives a larger TWLS in all three cases. In addition, for each disaster severity level, without support of DGs, electrical loads connected to child nodes of damaged power lines will be completely lost, leading to a higher total weighted power LS in Case C1 compared to Case B. Similarly, without emergency support of gas storages in the gas distribution system, total weighted gas LS also significantly increases in Case C2 compared to Case B. Furthermore, in Case C3 where no emergency response resource is available, the IENDS faces with the highest TWLS. It is concluded that DGs and gas storage assets are valuable emergency response resources for reducing TWLS and enhancing resilience of IENDSs.

TABLE IV WORST-CASE DAMAGES WITH EMERGENCY RESOURCES

Severity level	B		C1		C2		C3	
	Power	Gas	Power	Gas	Power	Gas	Power	Gas
1	299.14	0.00	497.60	0.00	303.31	11.04	497.60	2.35
2	484.49	1534.52	497.60	1534.52	484.49	1894.52	497.60	1894.52
3	484.49	2053.45	497.60	2053.45	484.49	2663.45	497.60	2663.45
4	484.49	2303.45	497.60	2303.45	484.49	2663.45	497.60	2663.45
5	484.49	2552.22	497.60	2552.22	484.49	2663.45	497.60	2663.45

In addition, gas LS levels in Cases C2 and C3 are higher than that of B. In these two cases, DGs are utilized to support high-priority power demands when power supply from the main-grid is cut off. However, gas storage facilities are not available which further deteriorate the situation of insufficient gas supply. As a result, low-priority gas load at gas node 12 is partially shed, while gas-fired DG at gas node 14 converts natural gas into electric power to support high-priority power loads at power nodes 14-15 and 17.

Furthermore, taking disaster severity level of 3 as an example while considering DGs and gas storages (i.e., row 3 in Table III), gas levels of storage asset at gas nodes 5 and 11 are shown in Fig. 4. It is observed from Fig. 4 that gas fuel stored in storage facilities is effectively utilized in response to pipeline outages. Specifically, when worst-case outages of pipelines P1-2 and P8-9 happen, gas supply is completely cut off. Thus, gas levels of storage assets at gas nodes 5 and 11 are increased to their maximum capacities at hour 7 to prepare for the catastrophic event at hour 8. That is, gas fuel stored in these storages can be used later to supply gas loads when natural gas supply is cut off after hour 8. As a result, a total 140 kcf of natural gas from storage facilities is utilized during hours 8-24 and TWLS is reduced by 610 as compared to C2.

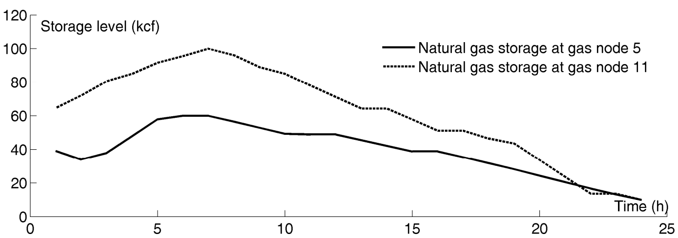

Fig. 4 Natural gas levels of gas storages

D. *Effectiveness of Network Hardening Strategies*

To demonstrate benefits of hardening strategies on IENDSs, TWLS with respect to different hardening budgets is studied with disaster severity level of 3. Coefficients of hardening effort of power lines and gas pipelines are set as 1 and 3, indicating that hardening an underground pipeline needs more efforts/cost than an overhead power line. Results in Table VI show that with a higher hardening budget, more power lines and pipelines will be hardened, leading to a smaller TWLS. Table VI also indicates that, as damaging pipelines could lead to higher TWLS, optimal hardening strategies prefer to harden gas pipelines with hardening budget smaller than 11. When hardening budget is sufficient (i.e., larger than 12), more power lines will be hardened in order to further reduce TWLS.

TABLE VI HARDENING STRATEGY AGAINST DIFFERENT HARDENING BUDGETS

Budget	Hardening Strategy	TWLS
1	L1-2	2474.87
2	L1-2, L2-3	2395.98
3	P8-9	2372.72
4	L1-2, P8-9	2309.66
5	L1-2, L6-7, P8-9	2268.00
6	P8-9, P9-10	1940.14
7	L1-2, P8-9, P9-10	1877.08
8	L1-2, L6-7, P8-9, P9-10	1835.42
9	P8-9, P9-10, P10-11	1750.15
10	L1-2, P8-9, P9-10, P10-11	1687.08
11	L1-2, L6-7, P8-9, P9-10, P10-11	1645.42
12	L1-2, L6-7, L7-8, P8-9, P9-10, P10-11	1603.76
13	L1-2, L2-3, L6-7, L7-8, P8-9, P9-10, P10-11	1572.91
14	L1-2, L2-3, L6-7, L7-8, L9-10, P8-9, P9-10, P10-11	1563.65

Hardening strategies in Table VI against different hardening budget levels also implicate importance of individual power lines and pipelines on system resilience. For instance, power line L1-2 is the most cirtical that would be hardened preferentially, as it is directly connected to the substation. Furthermore, pipelies P8-9, P9-10, and P10-11 are always hardened which indicates their importance in the IENDS. When hardening budget reaches 14, by optimally hardening 5 power lines and 3 pipelines, TWLS is decreased from 2474.87 to 1563.65 with a 37% drop. In addition, in this case, a proper budget level could be 6 because it brings the largest drop in TWLS of 327.85 for one unit increase in hardening budget.

E. *Sensitivity Analysis*

A sensitivity analysis on TWLS with respect to different hardening budgets and disaster severity levels is further performed, to illustrate their impacts on resilience of IENDSs. Results in Fig. 5 indicate a monotonically decreasing trend of TWLS with respect to an increase in hardening budgets and/or a decrease in disaster severity levels. Such a sensitivity study can guide utilities to determine proper hardening budgets for maintaining a certain resilience level of IENDSs in response to natural disasters of different disaster severity levels.

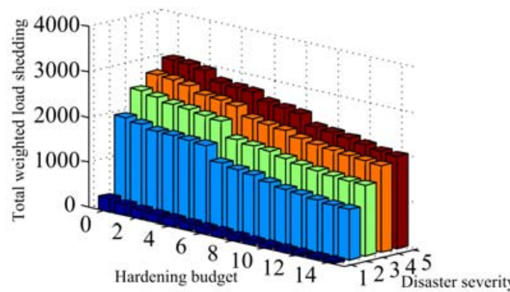

Fig. 5 TWLS under various hardening budgets and disaster severity levels

F. *Discussion on Computational Performance*

Computational performance of the proposed model is studied in this section. Table VII reports computational time and number of iterations with disaster severity level of 3. Overall, results show that number of iterations increases with the increase in hardening budget, because more hardening options are to be evaluated. In addition, numbers of iterations for budget levels of 6, 7, and 8 are lower because two important pipelines are always preferably hardened, which reduces the number of hardening options to be evaluated. The high computational time is mainly introduced by the CCG algorithm. That is, as the number of CCG iteration increases, numbers of variables and constraints increase, leading to a significant increase in computational time. In addition, Fig. 5 is derived in about four hours, which is sufficient for this type of offline applications to support timely and effective decision-making against natural disasters.

TABLE VII COMPUTATIONAL TIME WITH DISASTER SEVERITY LEVEL 3

Budget	Time(s)	# of iterations	Budget	Time(s)	# of iterations
1	5	3	8	35	8
2	6	3	9	154	14
3	16	6	10	183	15
4	80	11	11	220	16
5	128	13	12	257	17
6	10	4	13	492	23
7	26	7	14	981	34

V. Conclusion

This paper proposes a tri-level robust network hardening model for enhancing resilience of IENDSs against natural disasters. It provides optimal hardening strategies for proactively reinforcing power lines/ pipelines and minimizing the worst-case TWLS with respect to hardening budget limits and random damages caused by disasters of different severity levels. Distinct failure probabilities of overhead power lines and underground pipelines are considered. Furthermore, DGs and gas storage assets are considered as emergency response resources for supplying high-priority electricity/gas loads during disaster events and reducing TWLS. The proposed model is solved by CCG, in which nonlinear gas network constraints are linearized via Taylor series expansion. An iterative procedure is proposed to improve approximation accuracy of Taylor series expansion.

Numerical studies illustrate effectiveness of the proposed Taylor series expansion-based solution approach. It also shows that DGs and gas storage assets, as critical emergency response resources in IENDSs, could greatly reduce TWLS and enhance system resilience. Optimal network hardening strategies obtained from the proposed model can assist utilities in mitigating vulnerability of IENDSs against natural disasters.

References

[1] E. Blake, T. Kimberlain, R. Berg, J. Cangialosi, and J. Beven, Tropical Cyclone Report Hurricane Sandy (AL182012) 22-29 October 2012, National Hurricane Center, Feb. 2013.

[2] Y. Wang, C. Chen, J. Wang, and R. Baldick, "Research on resilience of power systems under natural disasters-A review," *IEEE Trans. Power Syst.*, vol. 31, no. 2, pp. 1604-1613, Mar. 2016.

[3] National Oceanic and Atmospheric Administration, Billion-Dollar Weather and Climate Disasters, 2014, [Online]. Available: http://www.ncdc.noaa.gov/billions/events.

[4] DoE, Comparing the Impacts of Northeast Hurricanes on Energy Infrastructure, 2013, [Online]. Available: https://energy.gov/oe/downloads/comparing-impacts-northeast-hurricanes-energy-infrastructure-april-2013.

[5] M. Ouyang, L. Dueñas-Osorio, "Multi-dimensional hurricane resilience assessment of electric power systems," *Structure Safety*, vol. 48, pp. 15-24, May. 2014.

[6] Executive Office of the President, Economic Benefits of Increasing Electric Grid Resilience to Weather Outages, 2013, [Online]. Available: https://energy.gov/downloads/economic-benefits-increasing-electric-grid-resilience-weather-outages.

[7] Edison Electric Institute, Before and After the Storm, 2014, [Online]. Available: https://http://www.eei.org/issuesandpolicy/electricreliability/mutualassistance/Documents/BeforeandAftertheStorm.pdf.

[8] DoE, Hardening and Resiliency: U.S. Energy Industry Response to Recent Hurricane Seasons, 2010, [Online]. Available: https://energy.gov/oe/downloads/hardening-and-resiliency-us-energy-industry-response-recent-hurricane-seasons-august.

[9] N. Romero, N. Xu, L. Nozick, I. Dobson, and D. Jones, "Investment planning for electric power systems under terrorist threat," *IEEE Trans. Power Syst.*, vol. 27, no. 1, pp. 108-116, Feb. 2012.

[10] N. Romero, L. Nozick, I. Dobson, N. Xu, and D. Jones, "Transmission and generation expansion to mitigate seismic risk," *IEEE Trans. Power Syst.*, vol. 28, no. 4, pp. 3692-116, Nov. 2013.

[11] W. Yuan, L. Zhao, and B. Zeng, "Optimal power grid protection through a defender-attacker-defender model," *Rel. Eng. Syst. Safety*, vol. 121, pp. 83-89, Jan. 2014.

[12] P. Kuntz, R. Christie, and S. Venkata, "Optimal vegetation maintenance scheduling of overhead electric power distribution systems," *IEEE Trans. Power Deli.*, vol.17, no.4, pp.1164-1169, Oct. 2002.

[13] A. Salman, Y. Li, and M. Stewart, "Evaluating system reliability and targeted hardening strategies of power distribution systems subjected to hurricanes," *Reliability Engineering & System Safety*, vol. 144, pp. 319-333, Aug. 2015.

[14] W. Yuan, J. Wang, F. Qiu, C. Chen, C. Kang, and B. Zeng, "Robust optimization-based resilient distribution network planning against natural disasters," *IEEE Trans. Smart Grid*, vol. 7, no. 6, pp. 2817-2826, Nov. 2016.

[15] S. Ma, B. Chen, and Z. Wang, "Resilience enhancement strategy for distribution systems under extreme weather events," *IEEE Trans. Smart Grid*, (to appear).

[16] EIA, Monthly Energy Review, 2016, [Online]. Available: http://www.eia.gov/totalenergy/data/monthly/#naturalgas/.

[17] G. Cimellaro, O. Villa, and M. Bruneau, "Resilience-based design of natural gas distribution networks," *J. Infrastruct. Syst.*, vol. 21, no. 1, pp. 1-14, 2014.

[18] E. Gil and J. McCalley, "A US energy system model for disruption analysis: Evaluating the effects of 2005 hurricanes," *IEEE Trans. Power Syst.*, vol. 26, no. 3, pp. 1040-1049, 2011.

[19] M. Ouyang and Z. Wang, "Resilience assessment of interdependent infrastructure systems: With a focus on joint restoration modeling and analysis," *Reliab. Eng. Syst. Saf.*, vol. 141, pp. 74-82, 2015.

[20] C. Shao, M. Shahidehpour, X. Wang, X. Wang, and B. Wang, "Integrated planning of electricity and natural gas transportation systems for enhancing the power grid resilience," *IEEE Trans. Power Syst.*, vol. 32, no. 6, pp. 4418-4429, Nov. 2017.

[21] C. Wang, W. Wei, J. Wang, F. Liu, F. Qiu, C. Correa-Posada, and S. Mei, "Robust defense strategy for gas-electric systems against malicious attacks," *IEEE Trans. Power Syst.*, vol. 32, no. 4, pp. 2953-2965, Jul. 2017.

[22] C. Borges and D. Falcão, "Optimal distributed generation allocation for reliability, losses, and voltage improvement," *Int. J. Elect. Power Energy Syst.*, vol. 28, no. 6, pp. 413-420, 2006.

[23] P. Georgilakis and N. Hatziargyriou, "Optimal distributed generation placement in power distribution networks: models, methods, and future research," *IEEE Trans. Power Syst.*, vol. 28, no. 3, pp. 3420-3428, Aug. 2013.

[24] EIA, Impact of the 2008 Hurricanes on the Natural Gas Industry, 2008, [Online]. Available: https://www.eia.gov/pub/oil_gas/natural_gas/feature_articles/2009/nghurricanes08/nghurricanes08.pdf.

[25] G. Pettit and B. Morgan, "A tool to estimate the failure rates of cross-country pipelines," *in Hazards XXI: Process Safety and Environmental Protection in a Changing World*. London, pp. 294-302, 2009.

[26] B. Zeng and L. Zhao, "Solving two-stage robust optimization problems using a column-and-constraint generation method," *Operations Research Lett.*, vol. 41, no. 5, pp. 457-461, 2013.

[27] A. Tomasgard, F. Rømo, M. Fodstad, and K. Midthun, "Optimization models for the natural gas value chain," *Geom. Model., Numer. Simul., Optimiz.*, pp. 521-558, 2007.

[28] C. Chen, J. Wang, F. Qiu, and D. Zhao, "Resilient distribution system by microgrids formation after natural disasters," *IEEE Trans. Smart Grid*, vol. 7, no. 2, pp. 958-966, Mar. 2016.

[29] M. Manbachi and M. Haghifam, "The economical feasibility of combined heat and power systems in energy markets based on reliability, using dynamic game theory," *Energy Sources, Part B: Econ., Planning, Policy*, vol. 10, pp. 82-90, Aug. 2015.

[30] Z. Wang, B. Chen, J. Wang, J. Kim, and M. Begovic, "Robust optimization based optimal DG placement in microgrids," *IEEE Trans. Smart Grid*, vol. 5, no. 5, pp. 2173-2182, Sep. 2014.

[31] M. Rice and S. Shenoi, Critical Infrastructure Protection X: 10th IFIP WG 11.10 International Conference, ICCIP 2016, Arlington, VA, USA, March 14-16, 2016, Revised Selected Papers. Springer, 2016.

[32] C. He, L. Wu, T. Liu, and M. Shahidehpour, "Robust co-optimization scheduling of electricity and natural gas systems via ADMM," *IEEE Trans. Sustain. Ener.*, vol. 8, no. 2, pp. 658-670, Apr. 2017.

[33] A. Martinez-Mares and C. Fuerte-Esquivel, "A unified gas and power flow analysis in natural gas and electricity coupled networks," *IEEE Trans. Power Syst*., vol. 27, no. 4, pp. 2156-2166, Nov. 2012.

[34] S. Wu, R. Rios-Mercade, E. Boyd, and L. Scott, "Model relaxation for the fuel cost minimization of steady-state gas pipeline networks," *Math. Comput. Model.,* vol. 31, no. 2-3, pp. 197-220, Jan. 2000.

[35] M. Qadrdan, M. Abeysekera, M. Chaudry, J. Wu, and N. Jenkins, "Role of power-to-gas in an integrated gas and electricity system in Great Britain," *Int. J. Hydrog. Energy*, vol. 40, no. 17, pp. 5763-5775, May 2015.

[36] Energy Star, Portfolio manager technical reference: thermal conversion

factors, 2015. [Online]. Available: https://www.energystar.gov/buildings/tools-and-resources/portfolio-manager-technical-reference-thermal-conversion-factors.

[37] R. Billinton and R. Allan, Reliability Assessment of Large Electric Power Systems. Boston, MA: Kluwer, 1988.

[38] C. Canham, M. Papaik, and E. Latty, "Interspecific variation in susceptibility to windthrow as a function of tree size and storm severity for northern temperate tree species," *Canadian Journal of Forest Research*, vol. 31, no. 1, pp. 1-10, Jan. 2001.

[39] L. Xu, "Underground assessment phase 3 report Ex Ante cost and benefit modeling," Quanta Tech., Raleigh, NC, Tech. Rep., May. 2008 [Online]. Available: http://www.feca.com/PURCPhase3FinalReport.pdf.

[40] H. Yeh, D. Gayme, and S. Low, "Adaptive VAR control for distribution circuits with photovoltaic generators," *IEEE Trans. Power Syst*., vol. 27, no. 3, pp. 1656-1663, Aug. 2012.

[41] L. Gan, N. Li, U. Topcu, and S. H. Low, "Exact convex relaxation of optimal power flow in radial networks," *IEEE Trans. Automat. Contr.*, vol. 60, no. 1, pp. 72-87, Jan. 2015.

[42] M. Farivar and S. H. Low, "Branch flow model: relaxations and convexification—Part I," *IEEE Trans. Power Syst*., vol. 28, no. 3, pp. 2554-2564, Aug. 2013.

[43] Z. Wang, B. Chen, J. Wang, and C. Chen, "Networked microgrids for selfhealing power systems," *IEEE Trans. Smart Grid*, vol. 7, no. 1, pp. 310-319, Jan. 2016.

[44] E. Menon, Gas Pipeline Hydraulics. Boca Raton, FL, USA: Taylor & Francis, 2005.

[45] K. Midthun, M. Bjørndal, and A. Tomasgard, "Modeling optimal economic dispatch and system effects in natural gas networks," *Energy J.*, vol. 30, no. 4, pp. 155-180, 2009.

[46] C. Floudas*, Nonlinear and Mixed-Integer Optimization: Fundamentals and Applications*, New York, NY, USA: Oxford Univ. Press, 1995.

[47] F. Romo, A. Tomasgard, L. Hellemo, M. Fodstad, B. Eidesen, and B. Pedersen, "Optimizing the Norwegian natural gas production and transport," *Interfaces*, vol. 39, no. 1, pp. 46-56, 2009.

[48] http://people.clarkson.edu/~lwu/data/Hardening/.

BIOGRAPHIES

Chuan He (S'13) received the B.S. degree, M.S. degree and Ph.D. degree in electrical engineering from Sichuan University, Chengdu, China in 2011, 2014 and 2018, respectively. He was a visiting Ph.D. student at Clarkson University, Potsdam, NY, USA from 2015 to 2017. He is currently an Associate Research Professor with the College of Electrical Engineering and Information Technology, Sichuan University, Chengdu, China. His research interests include robust optimization on power system operation and planning with renewable energy.

Chenxi Dai (S'15) received the B.E. degree from Zhejiang University, Hangzhou, China in 2011, and the M.S. degree from the University of Texas at Austin, USA, in 2013, both in Electrical Engineering. Currently he is pursuing Ph.D. degree in Electrical Engineering at Clarkson University, Potsdam, NY, USA. He has an internship with Economic Planning group at New York Independent System Operator (NYISO) in 2013. His research interests include robust optimization on power system operation and planning.

Lei Wu (SM'13) received the B.S. degree in electrical engineering and the M.S. degree in systems engineering from Xi'an Jiaotong University, Xi'an, China, in 2001 and 2004, respectively, and the Ph.D. degree in electrical engineering from Illinois Institute of Technology (IIT), Chicago, IL, USA, in 2008. From 2008 to 2010, he was a Senior Research Associate with the Robert W. Galvin Center for Electricity Innovation, IIT. He worked as summer Visiting Faculty at NYISO in 2012. Currently, he is an Associate Professor with the Electrical and Computer Engineering Department, Clarkson University, Potsdam, NY, USA. His research interests include power systems operation and planning, energy economics, and community resilience microgrid.

Tianqi Liu (SM'16) received the B.S. and the M.S. degrees from Sichuan University, Chengdu, China, in 1982 and 1986, respectively, and the Ph.D. degree from Chongqing University, Chongqing, China, in 1996, all are in Electrical Engineering. Currently, she is a professor in school of electrical engineering and information at Sichuan University. Her main research interests are power system analysis and stability control, HVDC, optimal operation, dynamic security analysis, dynamic State Estimation and load forecast.